Applied Catalysis A: General 447–448 (2012) 74–80

Contents lists available at SciVerse ScienceDirect

Applied Catalysis A: General

journal homepage: www.elsevier.com/locate/apcata

Inactivation path during the copper (II) catalyzed synthesis of Questiomycin A from oxidation of 2-aminophenol

Cătălina Olmazu[a], Mihaela Puiu[a,b,*], Irina Babaligea[a], Adina Răducan[a], Dumitru Oancea[a]

[a] Department of Physical Chemistry, University of Bucharest, 4-12 Elisabeta Boulevard, 030018, Bucharest, Romania
[b] LaborQ, University of Bucharest, 4-12 Elisabeta Boulevard, 030018 Bucharest, Romania

ARTICLE INFO

Article history:
Received 3 July 2012
Received in revised form 9 August 2012
Accepted 5 September 2012
Available online 14 September 2012

Keywords:
2-Aminophenol
Oxidation
Questiomycin A
Kinetic modelling
Copper(II) complex

ABSTRACT

The catalytic oxidation of 2-aminophenol (OAP) to 2-amino-3H–phenoxazin-3-one (APX, Questiomycin A) was the object of numerous studies partly due to antimicrobial properties of Questiomycin A and mostly because it can be used as a model for the synthesis of the naturally occurring antineoplastic agent Actinomycin D. Several copper complexes were used as dioxygen and/or substrates activators in order to mimic the activity of phenoxazinone synthase, but the reported assays failed to provide reasonable mechanistic features in media compatible with natural conditions. The main purposes of our work were to use simple copper salts to perform oxidation of OAP in oxygenated aqueous solutions and to develop a reaction scheme able to explain the low yields in APX along with the operational inactivation of the catalyst. A 11-step kinetic model able to describe the inactivation of copper(II) catalyst during oxidation of OAP to APX in oxygenated solutions was developed, and the rate constants for both catalytic and non-catalytic branch were estimated either experimentally or using a computing program for detailed kinetic simulation. It was demonstrated that the inactivation path can be assigned to formation of the stable bis(*o*-iminosemiquinonato)copper(II) complex, a compound reported as a moderate antimicrobial agent.

1. Introduction

Catalytic activation of dioxygen by copper ions in selective oxidations of organic compounds was paid considerable attention over at least four past decades mostly due to the abundance of copper in biological systems [1–3]. Copper-containing enzymes are usually acting as oxygen carriers in oxidation reactions of a large variety of substrates (carbohydrates, amines, phenols etc.) [4,5]. The role of copper centers in these enzymes, along with their detailed structure, is not entirely elucidated at present and may differ from enzyme to enzyme [6,7]. Mimicking systems using copper complexes as dioxygen and/or substrates activators were widely studied for understanding the complex pathways and mechanistic features of biological oxidations [8–12]. In this context, the oxidative coupling of 2-aminophenol (OAP) to the stable product, 2-amino-3H-phenoxazin-3-one (APX) through catalytic activation of dioxygen/substrate was the subject of numerous studies [13–15] partly due to antimicrobial properties of APX (also known as Questiomycin A) but mostly because it can be used as a model for the synthesis of the naturally occurring antineoplastic agent Actinomycin D [16].

Many works were dedicated in the past years to synthesis, characterization of copper-, iron-manganese and cobalt (II) complexes which were used to mimic the activity of phenoxazinone synthase (PHS) [5,9,13], a two-copper centre oxidase isolated from *Streptomyces* [7] which catalyzes the oxidation of substituted 2-aminophenols to the phenoxazinone chromophore in the final step of the Actinomycin D biosynthesis. It is now widely accepted that the six-electron oxidative condensation of two molecules of OAP to form APX occurs via 2-aminophenoxyl free radicals [15,17,18]. The generation of aminophenoxyl radical is supposed to occur catalytically or in the absence of the catalyst (auto-oxidation), but the following dismutation, addition, cyclization and oxidation steps do not require catalyst assistance [19] (Scheme 1).

It is worth mentioning several works which proposed copper(I) and (II) salts (CuCl, $CuCl_2$, $CuSO_4$, $Cu(NO_3)_2$, $Cu(OCH_3)_2$) and oxides (CuO, Cu_2O) [17,20] or Fe, Mn and Co(II) based complexes [5,13,21] as mimic systems of PHS activity; most of them provided conversions of OAP to APX up to 90% [20,21]. However, the main disadvantages of these assays are that the studies were achieved in organic solvents (acetonitrile, dimethylformamide, methanol) [13,15,20] at temperatures ranging from 40 to 60 °C [13,17,20], which are not compatible to the natural conditions where PHS displays its optimum activity [7]. Monocopper–dioxygen adducts

* Corresponding author at: Laboratory of Quality Control and Process Monitoring, University of Bucharest, 4-12 Regina Elisabeta Boulevard, 030018 Bucharest, Romania. Tel.: +40 21 4104888; fax: +40 21 4104888.
E-mail address: elenamihaela.puiu@g.unibuc.ro (M. Puiu).

0926-860X/$ – see front matter © 2012 Elsevier B.V. All rights reserved.
http://dx.doi.org/10.1016/j.apcata.2012.09.009

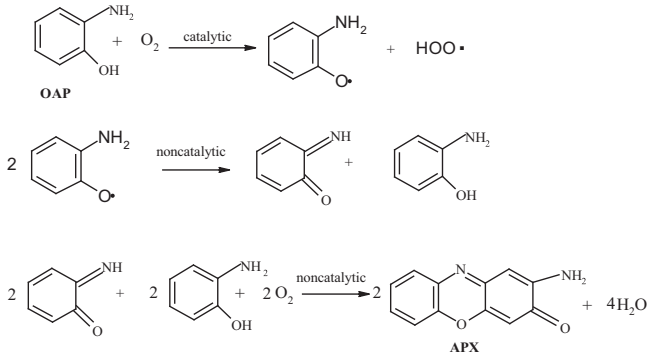

Scheme 1. Simplified model of kinetically significant oxidation steps of OAP.

have been postulated as intermediates in enzyme catalysis (notable examples being dopamine β-monooxygenase and galactose oxidase [22]), formulated as Cu(II) superoxo species [23]. Their structures were demonstrated kinetically, spectroscopically and by X-ray crystallography [8,22]. Many synthetic copper–oxygen adducts were prepared following the activation of dioxygen when binding to Cu(I) complexes with β-diketiminate ligands in order to explain/predict the existence of several active intermediates and the mechanistic features in copper catalyzed/mediated oxidations of organic compounds [22,24]. In this work we proposed and developed a reaction sequence for Cu(II) catalyzed oxidation of OAP which includes as plausible active intermediates Cu(II) superoxo species and Cu–OAP complexes, whose occurrence is sustained in literature data [4,23]. An inactivation step, assigned to the formation of the stable bis(*o*-iminosemiquinonato)copper(II) complex (also described in literature [4]), was added and experimentally checked. The Cu(II)-catalyzed oxidation of OAP being followed in air or dioxygen saturated solutions, the kinetic model took into account the reactions involving dissolved dioxygen according to the overall stoichiometry (Scheme 2):

The proposed model takes into account the generation of reactive oxygen species (ROS) such as $HOO^{\bullet}$, $HO^{\bullet}$ and other highly reactive radical species and starts with a set of rate constants reported in literature for 2-aminophenol oxidation [18,19] and generation of ROS species [25,26], others being obtained using an optimization algorithm.

2. Experimental

2.1. Materials

OAP was obtained from Aldrich Chemical Co. APX (m.p. = 249 °C) was synthesized upon the oxidation of 2-aminophenol with mercury oxide followed by recrystallization from ethanol, as described in several works [18,20]. Argon and gaseous dioxygen were purchased from Linde (99.9% purity for argon, 99.6% for dioxygen). Copper(II) salts: chloride, sulphate and acetate were of the highest purity grade from Fluka. Other chemicals used were of analytical reagent grade.

2.2. Apparatus

The ultraviolet–visible (Uv–Vis) measurements during the copper-catalyzed oxidation of OAP were made on a Lambda 25 Perkin-Elmer spectrophotometer with a Peltier cell for temperature and stirring control. The infrared (IR) spectra of solid OAP, APX and bis(*o*-iminosemiquinonato)copper(II) complex were recorded in the wavelength range 4000–400 cm^{-1} at room temperature in

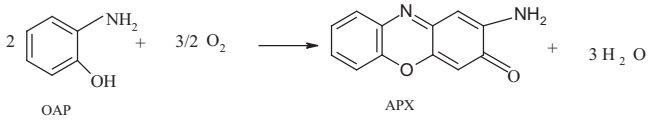

Scheme 2. Overall equation of OAP oxidation to APX.

KBr pellets on a BrukerTensor 37 spectrophotometer. High performance liquid chromatography (HPLC) analysis of reaction mixtures was performed on a HPLC-DAD system Agilent 1100 using a RP chromatographic column Kinetex C18Phenomenex 100 mm length and 2.1 mm inner diameter.

2.3. Synthesis of bis(o-iminosemiquinonato)copper(II) complex

The bis(*o*-iminosemiquinonato)copper(II) complex was obtained as described in literature [4]: the solution of Cu(II) salt was added in small portions to the ligand solution under continuous stirring, so that the complexation always took place with the excess OAP present. Each solution of 0.050 mM $CuCl_2$/$CuSO_4$/$Cu(CH_3COO)_2$ in 10 ml of water was added dropwise to a colourless solution of 0.100 mM of OAP dissolved in 10 ml of ethanol (molar ratio Cu(II):OAP = 1:2). As OAP can be rapidly oxidized by oxygen, in order to prevent the production of *o*-iminosemiquinones, an argon stream was bubbled through the solutions during the synthesis to ensure the absence of oxygen. Coloured precipitates of Cu(II) complex formed instantaneously. After 1.5 h stirring they were collected, washed with ethanol and water and dried. The highest conversion of the Cu(II) salt to Cu(II) complex was observed in the case of $Cu(CH_3COO)_2$ (60–70%) while the lowest conversion was obtained for $CuCl_2$ (10–15%).

2.4. Kinetic assays

The stability of OAP in the absence of oxygen was verified by passing an argon stream through the reaction mixture, when no significant transformation of OAP was observed. The initial concentration of OAP in the reactor ranged within 1×10^{-4} and 3×10^{-3} M, due to the low solubility in water of OAP and APX. Chemical transformation of the substrate was monitored by product (APX) analysis. For each experiment, 14–20 samples were removed from reactor at different time intervals and the spectra of the reaction mixture were recorded between 200 and 800 nm. HPLC analysis of the reaction mixture indicates as the main reaction product APX, other intermediates being accumulated in insignificant amounts towards OAP and APX. The validity of Dalton's law was assumed when calculating the concentration of dioxygen in saturated aqueous solution [27]. The air or dioxygen stream was bubbled through two thermostated saturation vessels containing water to avoid the evaporation of the solvent from reactor. Under these conditions the solution was saturated with dioxygen. All kinetic assays were run at 30 °C. APX formation was monitored measuring the absorbance at 434 nm (where OAP has no significant absorption) of the output sample (ε = 23,200 cm^{-1} M^{-1} for APX) [14]. The pH of each reaction mixture, established after copper salt addition, was also monitored in the output stream, but no significant deviation from the initial value (pH = 5.9–6.0) was noticed. Similar kinetic runs, carried out in the absence of catalyst, indicated a significant transformation with the formation of the same product. For the evaluation of the kinetic parameters involved in the catalytic reaction mechanism, the derivative d[APX]/dt assigned to the reaction rate of the catalytic branch was obtained by subtracting the reaction rate of the non-catalytic oxidation of OAP from the overall reaction rate at the same conversion.

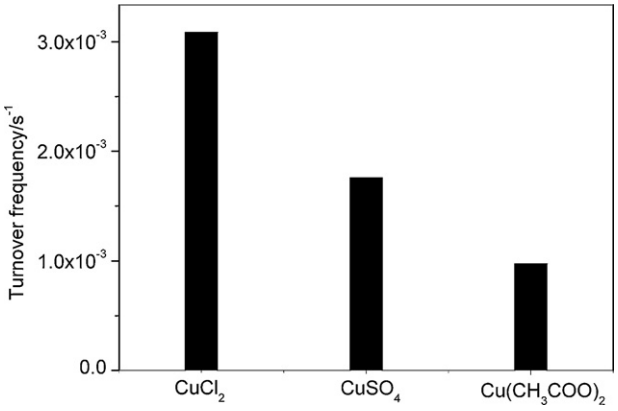

Fig. 1. Turnover frequency for three copper(II) salts: $[CuCl_2]_0$, $[CuSO_4]_0$, $[Cu(CH_3COO)_2]_0 = 1 \times 10^{-5}$ M, $[OAP]_0 = 1 \times 10^{-3}$ M, $T = 30\,^{\circ}C$.

3. Results and discussion

It was observed that APX was obtained according to the mass balance given by the stoichiometric equation (Scheme 2). In these conditions OAP oxidation to APX catalyzed by copper salts can be treated as a single reaction.

The reaction rates in initial conditions (2% conversion) were calculated as the slopes of the linear parts of the extended kinetic curves [APX] towards time and the turnover frequencies were obtained by dividing the slopes values to salt concentrations (Fig. 1).

The catalytic efficiency introduced by different copper salts can be assigned to anion effects resulting in incomplete dissociation (copper acetate), ion pair formation (copper sulphate) and possibly to some specific interactions.

Taking into account that the highest catalytic efficiency was achieved with $CuCl_2$, the following kinetic assays were focused on oxidation of OAP catalyzed by this compound. It was observed that the plots of initial rates against initial concentrations of OAP in dioxygen-saturated solution exhibited a peak-shaped curve similar to substrate inhibition pattern in enzymatic assays (Fig. 2). A 90% catalytic conversion in dioxygen saturated solution was achieved after 150 min. while the non-catalytic conversion was around 30% in the same conditions. Compared to the high yields obtained in time ranges up to 10 min. using several Cu(II) complexes in non-aqueous media which were widely described in literature [5,14,15,17], the low yields observed in aqueous media provide another argument to sustain the hypothesis of a inactive catalyst–substrate complex formation.

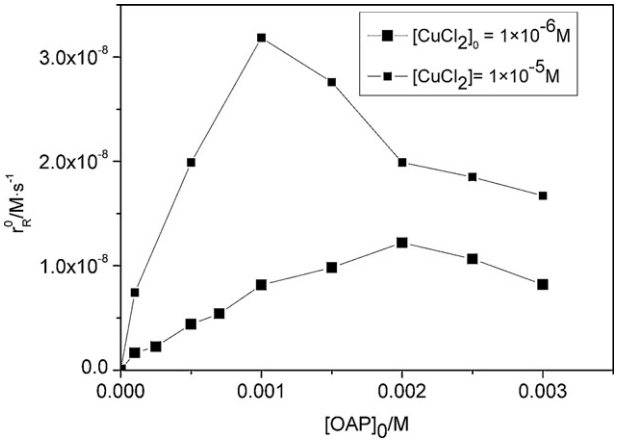

Fig. 2. Substrate inhibition of the initial reaction rate vs. initial concentration of substrate $[O_2]_{dissolved} = 1.17 \times 10^{-3}$ M, $T = 30\,^{\circ}C$.

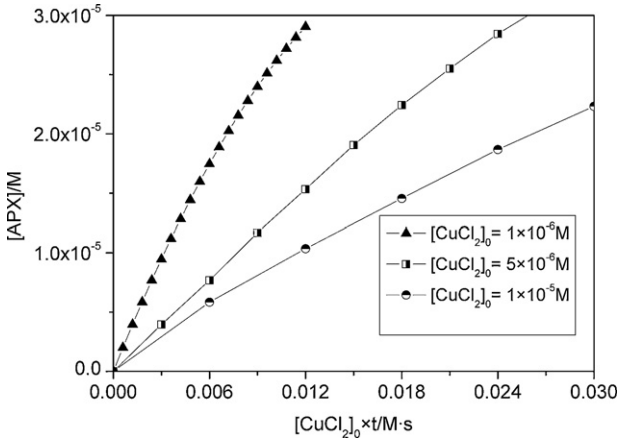

Fig. 3. Selwyn proof of catalyst inactivation: $[OAP]_0 = 1 \times 10^{-4}$ M, $[O_2]_{dissolved} = 1.17 \times 10^{-3}$ M, $T = 30\,^{\circ}C$.

The analysis of the extended progress curves (substrate or product concentration vs. time) allows checking the catalyst inactivation in excess of OAP, as in the case of the Selwyn test, originally conceived for the enzyme inactivation [19,28]. Accordingly, in the absence of inactivation, the graphs showing absorbance of APX (or an amount directly proportional to concentration of APX) versus the product $[Cu(II)]_0 \times$ time, for the same OAP concentration at several $[Cu(II)]_0$ concentrations, should be superposable, which was not observed in the studied system (Fig. 3).

The catalyst inactivation can be assigned to formation of bis(*o*-iminosemiquinonato)copper(II) complex $Cu(SH)_2$ (where SH is aminophenoxyl radical), which is formed upon the interaction of Cu(II) ions with OAP. The neutral square planar Cu(II) complex of the stoichiometry $Cu(SH)_2$ has been shown to be a diradical with a singlet ground state [4,29]. The complex was characterized upon its IR features against of those of OAP and APX, identifying the bands previously reported in literature for $Cu(SH)_2$ [4](Table 1).

3.1. Kinetic modelling

According to recent reported data about oxidation of OAP [6,9] and of several *o*-diphenols [2], an appropriate kinetic model can be developed comprising the generation of ROS species during the auto-oxidation of OAP in oxygenated solutions as well as formation of free radical products via catalytic steps. It is generally accepted that in solution Cu(II) is present as hexaaqua complex $(Cu(aq)_6)^{2+}$ and during the reaction steps of the catalytic branch it can be replaced by other ligands. In order to simplify the reaction sequence, the water molecules are omitted from the formulas of the involved copper(II) species.

$$SH_2 + Cu^{2+} \xrightarrow{k_1} (CuSH)^+ + H^+ \quad (1)$$

$$(CuSH)^+ + O_2 \xrightarrow{k_2} (CuO_2)^+ + SH^{\bullet} \quad (2)$$

$$(CuO_2)^+ \xrightarrow{k_3} Cu^{2+} + O_2^{\bullet -} \quad (3)$$

$$O_2^{\bullet -} + H^+ \xrightarrow{k_4} HOO^{\bullet} \quad (4)$$

$$SH_2 + O_2 \xrightarrow{k_5} SH^{\bullet} + HOO^{\bullet} \quad (5)$$

$$2SH^{\bullet} \xrightarrow{k_6} P \quad (6)$$

$$2HOO^{\bullet} \xrightarrow{k_7} H_2O_2 + O_2 \quad (7)$$

$$SH_2 + H_2O_2 \xrightarrow{k_8} SH^{\bullet} + HO^{\bullet} + H_2O \quad (8)$$

Table 1
IR spectral assignments of OAP, APX and Cu(II) complex (cm^{-1}).

Compound	$\tilde{\upsilon}$ (C—O)/cm^{-1}	$\tilde{\upsilon}$ (C—N)/cm^{-1}	$\tilde{\upsilon}$ (C=C)/cm^{-1}	$\tilde{\upsilon}$ (N—H)/cm^{-1}	$\tilde{\upsilon}$ (Cu—N)/cm^{-1}	$\tilde{\upsilon}$ (Cu—O)/cm^{-1}
OAP	1226	1283	1605	3304		
APX	1210	1273	1590	3413 3306		
$Cu(SH)_2$	1160	1296	1603	3286	620 422	599 526

$$H_2O_2 + HO^{\bullet} \xrightarrow{k_9} HOO^{\bullet} + H_2O \quad (9)$$

$$HOO^{\bullet} + H_2O_2 \xrightarrow{k_{10}} HO^{\bullet} + H_2O + O_2 \quad (10)$$

$$(CuSH)^+ + SH_2 \xrightarrow{k_{11}} Cu(SH)_2 + H^+ \quad (11)$$

where SH_2 is OAP. Occurrence of the active intermediate $(CuSH)^+$ is sustained by the formation (in absence of oxidizing agents) of the inactive complex ($Cu(SH)_2$). The formation of the highly reactive species $(CuO_2)^+$ is supported by recent reported data regarding the structure and reactivity of Cu(II)-superoxo adducts [22–24]. The assumption that ROS such as $HOO^{\bullet}$ and H_2O_2 are released during the auto-oxidation is also sustained by literature reported data [25,26] and from observed effects of copper(II) catalyst on OAP oxidation. In $CuCl_2$ aqueous solution copper is present as Cu^{2+}, $Cu(OH)^+$, $CuCl^+$, $CuCl_2$. The concentrations of these species were calculated solving the system of equations resulted from the equilibrium constants of formation ($\log K_{Cu(OH)^+} = -7.497$, $\log K_{Cu(Cl)^+} = 0.2$, $\log K_{CuCl_2} = -0.26$) [30] and the material balance equations, for $[CuCl_2]_0 = 1 \times 10^{-5}$ M and pH = 6.0. It was found that $(Cu(aq)_6)^{2+}$ is the most stable species (97%).

The simulation providing the kinetic behaviour of the entire system has to start from a particular set of rate constants and initial concentrations of the chemical species involved in the model. The rate constants found in literature are summarized in Table 2.

In addition, two rate constants (k_5 and k_8) were estimated experimentally following the experimental design and theoretical reasoning depicted in several previous works [18,19,31]. Briefly, an apparent first-order rate constant k'_5 was estimated by non-linear regression analysis after fitting an apparent first-order growth function on the progress kinetic curve [APX] vs. time obtained at the oxidation of OAP with dioxygen in dioxygen-saturated solution. The second-order rate constant k_5 was obtained as the ratio of k'_5 and $[O_2]$: $k_5 = (1.191 \pm 0.002) \times 10^{-2}\ M^{-1}\ s^{-1}$ with a significance level $\alpha = 0.05$. In a similar manner was obtained k_8, using the progress kinetic curve [APX] vs. time obtained during oxidation assay of OAP with hydrogen peroxide in a100-fold excess of H_2O_2: $k_8 = (2.011 \pm 0.006) \times 10^{-3}\ M^{-1}\ s^{-1}$ with a significance level $\alpha = 0.05$.

- Estimation of k_5: it was previously shown that the oxidation of OAP with dioxygen, in dioxygen saturated solution follows apparent first-order kinetics [18] with respect to substrate concentration. The partial reaction order towards dioxygen also being found equal to one [18,31] and taking into account Scheme 1 [5,14,20], we conclude that the rate determining step is the formation of aminophenoxyl radical.
- Estimation of k_8: as in the case of OAP auto-oxidation, the oxidation of OAP in the presence of H_2O_2 displays a second-order kinetics. Since the HPLC analysis of the reaction mixtures for both auto-oxidation OAP and oxidation with H_2O_2 proved that APX is the main reaction product and other intermediates are accumulated in insignificant amounts, steps (5) and (8) can be treated as single reactions, each being described by a single rate equation.

Table 2
Rate constants in aqueous medium used in the optimisation procedure.

Rate constant	Value/$M^{-1}\ s^{-1}$	Reference
k_7	1.6×10^5	[21,22]
k_9	2.7×10^7	[14]
k_{10}	0.50	[21]

The step 6 includes several fast elementary steps (dismutations, additions and oxidations occurring without catalyst assistance [15]); therefore, it can be treated as a single step in the specified working conditions (oxygen saturated solution). The constant k_6 was fixed at a plausible value of $1 \times 10^8\ M^{-1}\ s^{-1}$ because varying this parameter within 1×10^6–$1 \times 10^{10}\ M^{-1}\ s^{-1}$ (specific range of rate constant for fast reactions in solution) does not change the values of the optimised parameters.

- Estimation of k_{11} the inactivation step of the copper(II) catalyst assigned to formation of the inactive bis(*o*-iminosemiquinonato) copper complex can be pursued using an isoconversional method as described elsewhere for a first-order catalyst inactivation [28]. As long as the concentration of Cu(II) salt is much lower than the substrates concentrations OAP and O_2, a quasi-steady state is attained and the time evolution of the system can be described by a single overall reaction rate. The corresponding kinetic equation, based on the quasi-steady state or quasi-equilibrium assumptions, coupled with the catalyst molar balance, takes the general form:

$$\frac{d[APX]}{dt} = [Cu(II)]_0 \times f([APX]) \quad (12)$$

where $f([APX])$ is dependent only on the OAP conversion, if all other operational variables are held constant.

Within the isoconversional method, several kinetic runs are performed maintaining the initial concentrations of OAP and O_2 constant and varying $Cu(II)_0$ concentration. A family of extended progress curves [APX] as a function of time, for different $[Cu(II)]_0$ concentrations, is obtained. For a certain product concentration, resulted at the same OAP conversion, designated as $[APX]_{isoconv}$, different reaction times $t_1, t_2, t_3, \ldots$ can be measured on each curve, corresponding to $[Cu(II)]_{0,1}, [Cu(II)]_{0,2}, [Cu(II)]_{0,3} \ldots$ concentrations. Arbitrary values of $[APX]_{isoconv}$ can be selected as long as they are present on all progress curves. At each point $[Cu(II)]_{0,i}$–t_i, the reaction rate $(d[APX]/dt)_i$ can be calculated numerically by fitting a convenient function (e.g. a polynomial) to each experimental progress curve and taking its first derivative. Eq. (12) takes the form:

$$\left(\frac{d[APX]}{dt}\right)_i = f([APX]_{isoconv}) \times [Cu(II)]^*_{0,i} \quad (13)$$

where $[Cu(II)]^*_{0,i}$ is the total copper(II) concentration for run i, active at time t_i, considering that the remaining part of the catalyst is converted into an inactive form. The time evolution of the active

catalyst can be approximated in this case from the catalyst molar balance:

$$[\mathrm{Cu(II)}]_0^* + [\mathrm{Cu(SH)_2}] = [\mathrm{Cu(II)}]_0 \quad (14)$$

where

$$[\mathrm{Cu(II)}]^* + [(\mathrm{CuSH})^+] + [(\mathrm{CuO_2})^+] = [\mathrm{Cu(II)}]_0^* \quad (15)$$

The terms $[(\mathrm{CuSH})^+]$ and $[(\mathrm{CuO_2})^+]$ can be calculated from the approximate steady-state conditions $\mathrm{d}[(\mathrm{CuSH})^+]/\mathrm{dt} \approx 0$ and $\mathrm{d}[(\mathrm{CuO_2})^+]/\mathrm{dt} \approx 0$, or:

$$k_1 \bullet [\mathrm{Cu(II)}]^* \bullet [\mathrm{SH_2}] = k_2 \bullet [(\mathrm{CuSH})^+][\mathrm{O_2}] + k_{11}[(\mathrm{CuSH})^+][\mathrm{SH_2}] \quad (16)$$

$$k_2[\mathrm{O_2}][(\mathrm{CuSH})^+] = k_3[(\mathrm{CuO_2})^+] \quad (17)$$

The equation system (15)–(17) allows calculating the concentrations of actives intermediates $(\mathrm{CuSH})^+$, and $(\mathrm{CuO_2})^+$ as well as the concentration of active unbound catalyst $\mathrm{Cu(II)}^*$ as function of the total concentration of active catalyst $\mathrm{Cu(II)}_0^*$. The formation rate of the inactive complex $\mathrm{Cu(SH)_2}$ can be written as:

$$\frac{\mathrm{d}[\mathrm{Cu(SH)_2}]}{\mathrm{dt}} = k_{11}[(\mathrm{CuSH})^+][\mathrm{SH_2}] \quad (18)$$

The concentration of the inactive complex can be calculated also from Eq. (14)

$$[\mathrm{Cu(SH)_2}] = [\mathrm{Cu(II)}]_0 - [\mathrm{Cu(II)}]_0^* \quad (19)$$

Deriving Eq. (19) with respect to time and equalling to Eq. (18) one obtains:

$$-\frac{\mathrm{d}[\mathrm{Cu(II)}]_0^*}{\mathrm{dt}} = k_{11}[(\mathrm{CuSH})^+][\mathrm{SH_2}] \quad (20)$$

where

$$[(\mathrm{CuSH})^+] = \frac{k_1k_3[\mathrm{Cu(II)}]_0^*[\mathrm{SH_2}]}{k_2k_3[\mathrm{O_2}] + [\mathrm{SH_2}](k_3k_{11} + k_1k_3 + k_1k_2[\mathrm{O_2}])} \quad (21)$$

Since the inactivation step (11) is much slower than the steps (1) and (2) it can be neglected in the steady-state condition (16) and consequently Eq. (20) becomes:

$$-\frac{\mathrm{d}[\mathrm{Cu(II)}]_0^*}{\mathrm{dt}} = \frac{k_1k_3k_{11}[\mathrm{SH_2}]^2[\mathrm{Cu(II)}]_0^*}{k_2k_3[\mathrm{O_2}] + (k_1k_3 + k_1k_2[\mathrm{O_2}])[\mathrm{SH_2}]} \quad (22)$$

No simple procedure exists to integrate this equation in order to obtain $[\mathrm{Cu(II)}]_0^*$ as a function of time when $[\mathrm{SH_2}]$ changes in time. However, two simpler limiting cases are obtained when one of the two terms in the denominator can be neglected.When $k_2k_3[\mathrm{O_2}] \ll (k_1k_3 + k_1k_2[\mathrm{O_2}])[\mathrm{SH_2}]$, Eq. (22) takes the following form:

$$-\frac{\mathrm{d}[\mathrm{Cu(II)}]_0^*}{\mathrm{dt}} = \frac{k_1k_3k_{11}[\mathrm{SH_2}]}{(k_1k_3 + k_1k_2[\mathrm{O_2}])}[\mathrm{Cu(II)}]_0^* \quad \text{or} \quad -\frac{\mathrm{d}[\mathrm{Cu(II)}]_0^*}{\mathrm{dt}} = \frac{k_{11}[\mathrm{SH_2}]}{\left(1 + \left(\frac{k_2}{k_3}\right)[\mathrm{O_2}]\right)}[\mathrm{Cu(II)}]_0^* \quad (23)$$

Integration of Eq. (23) after separating the variables, and taking into account that the concentration of the dissolved dioxygen was maintained constant during the oxidation assays, gives:

$$-\int_{[\mathrm{Cu(II)}]_0}^{\mathrm{Cu(II)}_0^*} \frac{\mathrm{d}[\mathrm{Cu(II)}]_0^*}{[\mathrm{Cu(II)}]_0^*} = \frac{k_{11}}{\left(1 + (k_2/k_3)[\mathrm{O_2}]\right)} \int_0^t [\mathrm{SH_2}]\mathrm{dt} \quad (24)$$

For i set, from $t = 0$ to isoconversional time, t_{isoconv} one obtains:

$$[\mathrm{Cu(II)}]_{0,i}^* = [\mathrm{Cu(II)}]_{0,i} \times e^{-k_{\mathrm{in1}}I_1} \quad (25)$$

where the inactivation constant k_{in1} and integral I_1 are:

$$k_{\mathrm{in1}} = \frac{k_{11}}{1 + (k_2/k_3)[\mathrm{O_2}]} \quad \text{and} \quad I_1 = \int_0^{t_{\mathrm{isoconv}}} [\mathrm{SH_2}]\mathrm{dt} \quad (26)$$

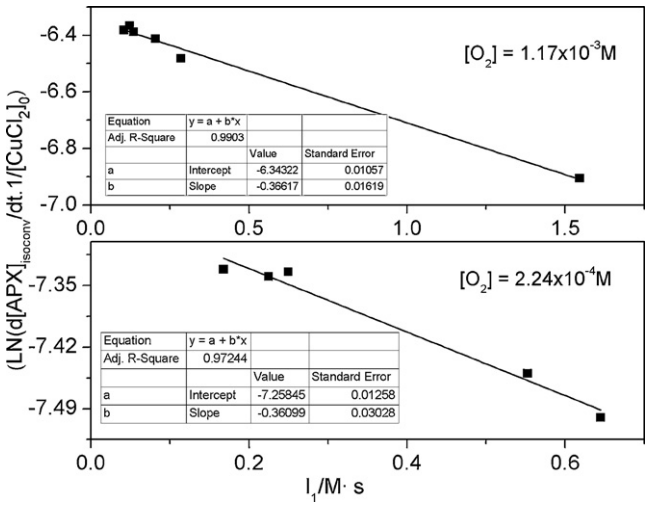

Fig. 4. Estimation of k_{in1} in dioxygen/air saturated solutions according to the first limiting case – Eqs. (25) and (26). $[\mathrm{OAP}]_0 = 1 \times 10^{-4}$ M, $T = 30\,^\circ$C, conversion ≈ 20%, $[\mathrm{CuCl_2}]_0$ ranging from 5×10^{-7} M to 1×10^{-6} M.

On the other hand, assuming that $k_2k_3[\mathrm{O_2}] \gg (k_1k_3 + k_1k_2[\mathrm{O_2}])[\mathrm{SH_2}]$, Eq. (22) becomes:

$$-\frac{\mathrm{d}[\mathrm{Cu(II)}]_0^*}{\mathrm{dt}} = \frac{k_1k_{11}[\mathrm{SH_2}]^2[\mathrm{Cu(II)}]_0^*}{k_2[\mathrm{O_2}]} \quad \text{or} \quad -\frac{\mathrm{d}[\mathrm{Cu(II)}]_0^*}{\mathrm{dt}} = \frac{k_1k_{11}[\mathrm{SH_2}]^2}{k_2[\mathrm{O_2}]}[\mathrm{Cu(II)}]_0^* \quad (27)$$

After integration one obtains:

$$[\mathrm{Cu(II)}]_{0,i}^* = [\mathrm{Cu(II)}]_{0,i} \times e^{-k_{\mathrm{in2}}I_2} \quad (28)$$

with

$$k_{\mathrm{in2}} = \frac{k_1k_{11}}{k_2[\mathrm{O_2}]} \quad \text{and} \quad I_2 = \int_0^{t_{\mathrm{isoconv}}} [\mathrm{SH_2}]^2\mathrm{dt} \quad (29)$$

The integrals I_1 and I_2 can be calculated numerically as the area under the curves [OAP] or $[\mathrm{OAP}]^2$ as functions of time, after fitting smooth functions (polynomials) on the experimental set of data of the form $[\mathrm{OAP}] = [\mathrm{OAP}]_0 - 2[\mathrm{APX}]$. Replacing the concentration of active catalyst from Eq. (25) in Eq. (13), one obtains:

$$\frac{(\mathrm{d}[\mathrm{APX}]/\mathrm{dt})_{i_{\mathrm{isoconv}}}}{[\mathrm{Cu(II)}]_{0,i}} = f([\mathrm{APX}]_{\mathrm{isoconv}}) \cdot e^{-k_{\mathrm{in1}}I_1} \quad (30)$$

The inactivation constant k_{in1} can be estimated using a nonlinear regression analysis of Eq. (30) with $(\mathrm{d}[\mathrm{APX}]/\mathrm{dt})_{\mathrm{isoconv}}/[\mathrm{Cu(II)}]_{0,i}$ as dependent variable, I_1 as independent variable and $f([\mathrm{APX}]_{\mathrm{isoconv}})$ and k_{in1} as estimated parameters, or using a linear regression analysis of the logarithmic form of the same equation. The evaluation of the inactivation kinetic constant k_{in1} is illustrated in Fig. 4:

Alternatively, replacing the concentration of the active catalyst from Eq. (28) in Eq. (13), one obtains:

$$\frac{(\mathrm{d}[\mathrm{APX}]/\mathrm{dt})}{[\mathrm{Cu(II)}]_{0,i}} = f([\mathrm{APX}]_{\mathrm{isoconv}}) \cdot e^{-k_{\mathrm{in2}}I_2} \quad (31)$$

Following the same procedure, the linear regression analysis of the logarithmic form of Eq. (31) is illustrated in Fig. 5. Both the derivatives $(\mathrm{d}[\mathrm{APX}]/\mathrm{dt})_i$ and integrals I_1 and I_2 have been calculated numerically.

The results for $k_{\mathrm{in}1}$ ($0.361 \pm 0.030\,\mathrm{s^{-1}}$ for $\mathrm{O_2}$ and $0.366 \pm 0.016\,\mathrm{s^{-1}}$ for air) and for k_{in2} ($4165 \pm 169\,\mathrm{s^{-1}}$ for $\mathrm{O_2}$ and $4023 \pm 342\,\mathrm{s^{-1}}$ for air) indicate an apparent independence of the inhibition of the dissolved oxygen concentration. The numerical integration and optimization of the rate constants involved in

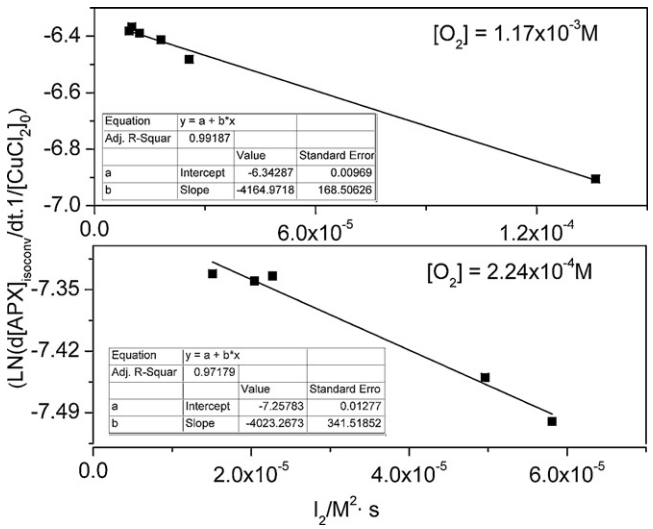

Fig. 5. Estimation of k_{in2} in dioxygen/air saturated solutions according to the second limiting case [Eqs. (28) and 29)]. $[OAP]_0 = 1 \times 10^{-4}$ M, $T = 30\,^{\circ}C$, conversion ≈ 20%, $[CuCl_2]_0$ ranging from 5×10^{-7} M to 1×10^{-6} M.

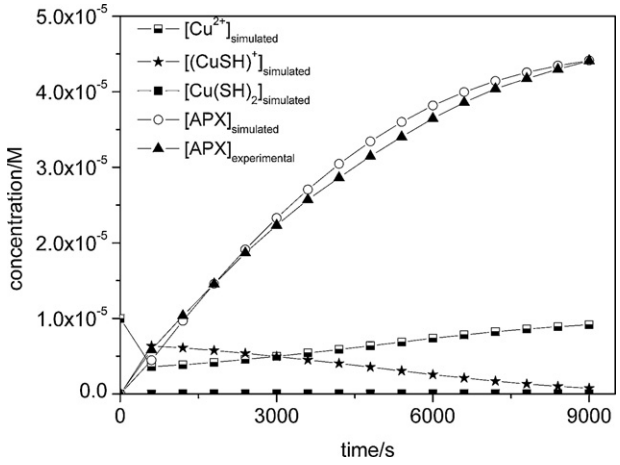

Fig. 6. Simulated and experimental extended kinetic curves of the reaction intermediate and products. $[OAP]_0 = 1 \times 10^{-4}$ M, $[O_2]_{dissolved} = 1.17 \times 10^{-3}$ M, $[CuCl_2]_0 = 1 \times 10^{-5}$ M, $T = 30\,^{\circ}C$.

the system of differential Eqs. (1)–(11) can help to discriminate between these limiting cases and to establish the significance of the inhibition constant.

3.2. Simulation assays

The time evolution of the reacting system was described by a set of differential equations obtained from the reaction steps 1–11, corresponding to the transformation rates for all species involved in the proposed model (except dioxygen whose concentration is kept constant in the working conditions). The optimisation process was accomplished with Kintecus [32] on 20 different experimental data sets.

3.3. Sensitivity analysis

The sensitivity analysis, accomplished with Atropos [33] at three different time intervals in order to avoid over-parameterization shows that all rate constants do influence the shape of the simulated progress curves and consequently all proposed steps can be considered kinetically significant. The optimized values are: $k_1 = (58.50 \pm 0.04)\,M^{-1}\,s^{-1}$, $k_2 = (2.18 \pm 0.04)\,M^{-1}\,s^{-1}$, $k_3 = (2.80 \pm 0.08) \times 10^2\,s^{-1}$, $k_4 = (5.100 \pm 0.024) \times 10^6\,M^{-1}\,s^{-1}$ and $k_{11} = (4.80 \pm 0.05) \times 10^{-2}\,M^{-1}\,s^{-1}$ (with $\alpha = 0.05$). The simulated progress curves for the proposed active and inactive copper species $(CuSH)^+$, $Cu(SH)_2$ together with both simulated and experimental kinetic curves for APX are displayed in Fig. 6, for substrate conversion around 90%. The agreement between experimental and simulated kinetic curves of APX was noticed likewise on the other experimental data sets.

The optimized parameters k_1, k_2, k_3, k_{11} and concentrations $[O_2]$ and $[SH_2]$ can be used to decide which terms in the denominator of Eq. (21) and those subsequently derived from it can be neglected. With present data Eq. (22) becomes simpler but still difficult to integrate:

$$-\frac{d[Cu(II)]_0^*}{dt} = \frac{k_1 k_{11}[SH_2]^2[Cu(II)]_0^*}{k_2[O_2] + k_1[SH_2]} \quad (32)$$

For air saturated solutions $k_2[O_2] \approx 4.9 \times 10^{-4}\,s^{-1}$ and $k_1[SH_2] \approx 5.9 \times 10^{-3}\,s^{-1}$. If the first term in the denominator is neglected as a rough approximation, one obtains $k_{in1} \approx k_{11}$, a result obtained also from Eq. (26) since $k_2[O_2]/k_3 = 1.7 \times 10^{-6} \ll 1$. This explains the apparent independence of the inhibition constant on the dioxygen concentration. For dioxygen saturated solution the approximation is even rougher but still in accord with the experimental behaviour. It can be concluded that only the first limiting approximation $k_2 k_3[O_2] \ll (k_1 k_3 + k_1 k_2[O_2])[SH_2]$, although rough, can explain the results, while the second one, predicting an inverse proportionality of the inhibition constant with the oxygen concentration is in disagreement with the results. The above approximations can partly explain the difference between the measured inhibition constant $k_{in1} = 0.366\,M^{-1}\,s^{-1}$ and calculated value $k_{11} = 0.048\,M^{-1}\,s^{-1}$.

4. Conclusions

The oxidation of 2-aminophenol with dissolved dioxygen in aqueous solution to give 2-amino-3H-phenoxazin-3-one is catalyzed by simple copper salts. The kinetics of the process indicates the existence of an inhibition by the substrate, confirmed by the characteristic variation of the initial reaction rate with substrate concentration, which presents a maximum, and also by the Selwyn test. A kinetic model implying 11 steps (catalytic and non-catalytic) was proposed, where the inhibition step represents the formation of bis(*o*-iminosemiquinonato)copper(II) complex, isolated and characterized. Several rate constants of the component steps were taken from literature and the others were evaluated either experimentally or numerically using an optimization procedure according to Kintecus software. The inhibition constant was also evaluated using an isoconversional procedure described earlier. The agreement between the measured and simulated inhibition constant proves that this method can rapidly provide mechanistic insights of the studied system and accurately describe the time evolution of active intermediates or side reaction products. The relative simple and costly-efficient manner to detect and evaluate the degree of operational inactivation of a catalyst in homogenous media is suitable for routine analysis in batch/flow reactors where the output signal of a stable reaction product can be measured, even when dealing with a single reaction or with a reaction network.

Acknowledgements

This work was supported by the strategic grant POSDRU/89/1.5/S/58852 project "Postdoctoral programme for training young scientific researchers", co-financed by the European Social

Fund within the Sectorial Operational Programme for Human Resources Development 2007–2013.

References

[1] M. Ahmed, Coord. Chem. Rev. 254 (2010) 1918–1947.
[2] G. Busca, S. Berardinelli, C. Resini, L. Arrighi, J. Hazard. Mater. 160 (2008) 265–288.
[3] J. Araña, V.M. Rodríguez López, E. Pulido Melián, M.I. Suárez Reyes, J.M. Doña Rodríguez, O. González Díaz, Catal. Today 129 (2007) 177–184.
[4] N.V. Loginova, T.y.V. Koval'chuk, R.A. Zheldakova, N.P. Osipovich, V.L. Sorokin, G.I. Polozov, G.A. Ksendzova, G.K. Glushonok, A.A. Chernyavskaya, O.I. Shadyro, Bioorg. Med. Chem. Lett. 16 (2006) 5403–5407.
[5] T.M. Simandi, L.I. Simandi, M. Gyor, A. Rockenbauer, A. Gomory, Dalton Trans. (2004) 1056–1060.
[6] W.A. Alves, S.A.d. Almeida-Filho, M.V.d. Almeida, A. Paduan-Filho, C.C. Becerra, A.M.D.C. Ferreira, J. Mol. Catal. A: Chem. 198 (2003) 63–75.
[7] M. Le Roes-Hill, C. Goodwin, S. Burton, Trends Biotechnol. 27 (2009) 248–258.
[8] G. Battaini, A. Granata, E. Monzani, M. Gullotti, L. Casella, Biomimetic oxidations by dinuclear and trinuclear copper complexes, in: R.v. Eldik, J. Reedijk (Eds.), Advances in Inorganic Chemistry, Academic Press, 2006, pp. 185–233.
[9] M.R. Maurya, S. Sikarwar, T. Joseph, S.B. Halligudi, J. Mol. Catal. A: Chem. 236 (2005) 132–138.
[10] M. Rolff, J. Schottenheim, G. Peters, F. Tuczek, Angew. Chem. Int. Ed. 49 (2010) 6438–6442.
[11] D. Li, Y. Tong, J. Huang, L. Ding, Y. Zhong, D. Zeng, P. Yan, J. Mol. Catal. A: Chem. 345 (2011) 108–116.
[12] M. Rolff, J. Schottenheim, H. Decker, F. Tuczek, Chem. Soc. Rev. 40 (2011) 4077–4098.
[13] M. Hassanein, M. Abdo, S. Gerges, S. El-Khalafy, J. Mol. Catal. A: Chem. 287 (2008) 53–56.
[14] J. Kaizer, R. Csonka, G. Speier, J. Mol. Catal. A: Chem. 180 (2002) 91–96.
[15] I.C. Szigyártó, T.M. Simándi, L.I. Simándi, L. Korecz, N. Nagy, J. Mol. Catal. A: Chem. 251 (2006) 270–276.
[16] S. Shimizu, M. Suzuki, A. Tomoda, S. Arai, H. Taguchi, T. Hanawa, S. Kamiya, Tohoku J. Exp. Med. 203 (2004) 47–52.
[17] L. Prati, M. Rossi, N. Ravasio, J. Mol. Catal. 75 (1992) 347–355.
[18] M. Puiu, A. Răducan, I. Babaligea, D. Oancea, Bioproc. Biosyst. Eng. 31 (2008) 579–586.
[19] M. Puiu, M. Constantinovici, I. Babaligea, A. Raducan, C. Olmazu, D. Oancea, Chem. Eng. Technol. 33 (2010) 414–420.
[20] T. Horváth, J. Kaizer, G. Speier, J. Mol. Catal. A: Chem. 215 (2004) 9–15.
[21] C. Mukherjee, T. Weyhermüller, E. Bothe, P. Chaudhuri, Compt. Rend. Chem. 10 (2007) 313–325.
[22] D. Maiti, H.C. Fry, J.S. Woertink, M.A. Vance, E.I. Solomon, K.D. Karlin, J. Am. Chem. Soc. 129 (2006) 264–265.
[23] A.M. Reynolds, B.F. Gherman, C.J. Cramer, W.B. Tolman, Inorg. Chem. 44 (2005) 6989–6997.
[24] N.W. Aboelella, S.V. Kryatov, B.F. Gherman, W.W. Brennessel, V.G. Young, R. Sarangi, E.V. Rybak-Akimova, K.O. Hodgson, B. Hedman, E.I. Solomon, C.J. Cramer, W.B. Tolman, J. Am. Chem. Soc. 126 (2004) 16896–16911.
[25] D.E.C. Benon, H.J. Bielski, A.B. Ross, J. Phys. Chem. Ref. Data 14 (1985) 1041–1100.
[26] I. Boutelet, S. Alexandre, J.-C. Vincent, Eur. J. Biochem. 223 (1994) 489–496.
[27] IUPAC Solubility Data Series in: Oxygen and Ozone, Pergamon Press, New York, 1981.
[28] D. Oancea, A. Stuparu, M. Nita, M. Puiu, A. Raducan, Biophys. Chem. 138 (2008) 50–54.
[29] N.V. Loginova, T.V. Koval'chuk, N.P. Osipovich, G.I. Polozov, V.L. Sorokin, A.A. Chernyavskaya, O.I. Shadyro, Polyhedron 27 (2008) 985–991.
[30] J.D. Allison, D.S. Brown, K.J. Novo-Gradac, A Geochemical Assessment Model for Environmental Systems: Version 4.0 User's Manual, in: MINTEQA2/PRODEFA2, United States Environmental Protection Agency, Office of Research and Development, Washington, DC, 1999.
[31] D. Oancea, M. Puiu, Cent. Eur. J. Chem. 1 (2003) 233–241.
[32] J.C. Ianni, Kintecus Windows Version 4.5. www.kintecus.com
[33] J.C. Ianni, ATROPOS, Windows Version 1.0, 2004. www.kintecus.com.